37th AIAA Plasmadynamics and Lasers Conference
5 - 8 June 2006, San Francisco, California

AIAA 2006-2891

Local Dynamic Subgrid Closure for Compressible MHD Turbulence Simulation

Kenji Miki[*] and Suresh Menon[†]
Georgia Institute of Technology,
Atlanta, GA, 30332-0150,
USA

A Local Dynamic Kinetic Energy Model (LDKM) for large-eddy simulation (LES) of magnetohydrodynamicis (MHD) turbulence is proposed. The proposed MHD turbulence model evaluates all model coefficients locally and dynamically without any *ad hoc* averaging. This model does not assume low magnetic Reynolds numbers. The turbulent residual-helicity effect (α-effect) appearing in the magnetic induction equation is successfully modeled and consistently remains a pseudo-scalar. This paper uses the MHD-LDKM LES model to compute high-Re decaying isotropic turbulence in a magnetic field. A decay model is used for validation. It is observed that the energy spectrum follows a $k^{-5/3}$ law in DNS and LDKM results. For further validation, the long time behavior of ideal invariants: energy (E), cross helicity (H_c), and magnetic helicity (H_m) are examined. The expected selective decay is observed when H_c is finite. This MHD LDKM model is applicable to wide variety of high/low magnetic Reynolds number applications.

Nomenclature

$(*)^{sgs}$	subgrid scale value
α-effect	force to generate a poloidal electric current from the poloidal magnetic field
$\bar{\Omega}_k$	resolved vorticity
$\bar{a}_{ij}$	resolved part of MHD shear stress
$\bar{B}_i$	resolved magnetic field
$\bar{M}_{ij}$	resolved rate of magnetic strain
β	turbulent closure coefficient
ϵ^b	magnetic dissipation term
ϵ^v	kinetic dissipation term
ϵ_{ijk}	alternating tensor
$\hat{f}$	test filtered
$k^{sgs,b}$	subgrid magnetic energy
k^{sgs}	subgrid kinetic enregy
κ	thermal conductivity
λ	magnetic diffusivity
μ_b	permeability
ν	viscosity
ν_t^a	magnetic diffusivity related to $\tau_{ij}^{sgs,v,a}$
ν_t^v	turbulent viscosity
ν_e	effective viscosity
$\overline{\Delta}$	local grid width
ρ	density
σ	electric conductivity

[*]Graduate Research Assistant, AIAA Student Member.
[†]Professor, and AIAA Associate Fellow

$\sigma_i^{sgs,v}$	subgrid work
$\tau_{ij}^{sgs,b'}$	unresolved magnetic stress tensor
$\tau_{ij}^{sgs,b}$	magnetic Reynolds stress
$\tau_{ij}^{sgs,v,a}$	Reynolds stress related to $b_i^{'}b_j^{'}$
$\tau_{ij}^{sgs,v,v}$	Reynolds stress related to $u_i^{'}u_j^{'}$
$\tau_{ij}^{sgs,v}$	subgrid kinetic stress= $-(\tau_{ij}^{sgs,v,v} - \tau_{ij}^{sgs,v,a})$
τ_{ij}	viscous stress
$\tilde{A}_{ij}$	spacial filtered MHD shear stress
$\tilde{f}$	spacial filtered
$\tilde{S}_{ij}$	resolved rate of strain
A_{ij}	MHD shear stress
b_i'	fluctuating magnetic field
$C_\nu^{v,a}$	turbulent closure coefficient
$C_\nu^{v,v}$	turbulent closure coefficient
$C_{\epsilon,b}$	turbulent closure coefficient
C_ϵ	turbulent closure coefficient
E	total energy
E_T^k	turbulent electromotive force
H_i^{sgs}	subgrid heat enthalpy flux
k	kinetic energy
P	pressure
Pr_t	turbulent Prandtle number
q_i^{sgs}	subgrid heat flux vector
u	velocity
u'	fluctuating velocity
$\alpha^{'}$	turbulent closure coefficient

I. Introduction

Numerical simulation is a powerful tool to understand the fundamental aspects of MHD turbulence. The linear and nonlinear coupling of the fluid motion with the magnetic field complicates the development of an accurate model. The term $\epsilon_{kij}u_iB_j$, derivative of the Lorentz force, is similar to the Reynolds stress term dealt with in conventional LES turbulence modeling. Here, u_i is the velocity, B_j is the magnetic field, and ϵ_{kij} is the alternating tensor. This nonlinear coupling term has been extensively studied in the past, and many approaches for closure of this term have been proposed.[1–6] A detailed discussion of this term and the α-effect is given by Yoshizawa.[7–9] The α-effect generates a poloidal electric current from the poloidal magnetic field and is one of the key turbulent dynamo features.

In three-dimensional MHD turbulence, there are three invariants that play a critical role in the behavior of MHD turbulence.[10] These are the total energy $E^t = \int(u_ku_k + B_kB_k)dV = E^k + E^m$, the magnetic helicity $H_m = \int A_kB_kdV$, and the cross helicity $H_c = \int u_kB_kdV$, where $\mathbf{A}$ is the vector potential. The physical interpretations of H_m and H_c are following. H_m shows the measurement of topological linkage of magnetic field and is strongly related to the back-scatter mechanism by which the magnetic energy E^m is accumulated in the large scale (less dissipative) scales.[11] This is the so-called selective decay process.[12] In most real applications, a finite value of H_m is expected, which results in a slower decay of magnetic energy.

There are two important mechanisms related to H_c: the dynamic alignment process,[13] which forces the plasma flow velocity and the magnetic field to align, and the back-transfer of kinetic energy.[11] From a numerical viewpoint, H_c influences the model coefficients γ as seen in the turbulent electromotive force term E_T^k (defined later).[9]

The main objective of this study is to develop and validate a new dynamic SGS model for an electrically conducting fluid. The significance of this new model is that the closure of $\epsilon_{ijk}u_jB_k$ is computed directly under the well-studied assumption of similarity between the subgrid and test filtered scale dynamics.[14] A requirement for this study was that the model needed to account for the pseudo-vector nature of the magnetic field to ensure that closure contains information of both magnitude and direction (sign).

There are several other requirements that any accurate and efficient subgrid model must satisfy. First,

the modeling procedure should be easily incorporated into a well-established LES solver. Therefore, effort is made to reduce the introduction of unnecessary modeling coefficients. Second, the model should be applicable to numerous applications. As a result, neither the assumption of low magnetic Reynolds nor of homogeneous turbulence is made in order to simplify the derivation of the LES equations and the closure terms. Third, the model should not depend on *ad hoc* procedures. Therefore, the model coefficients are determined locally and dynamically instead of from experimental data. A MHD-LDKM model meeting these criteria is described in detail in Section II. Before the numerical results are presented, the constraint of $\partial B_i/\partial x_i = 0$ are examined in section III. This is a critical problem seen in many MHD calculations that use finite difference schemes. Preliminary results are shown in Section IV. Conclusions are summarized in Section V.

II. Governing Equations

A. Derivation of LES equations

An electrically conducting fluid is governed by the Navier-Stokes equations with the addition of a Lorentz force term in the momentum equation, a corresponding work term in the energy equation,

$$\frac{\partial \rho}{\partial t} = -\frac{\partial}{\partial x_j}(\rho u_j) \tag{1}$$

$$\frac{\partial \rho u_i}{\partial t} = -\frac{\partial}{\partial x_j}(\rho u_i u_j) - \frac{\partial P}{\partial x_i} + \frac{\partial \tau_{ij}}{\partial x_j} + \epsilon_{ijk} J_j B_k = -\frac{\partial}{\partial x_j}(\rho u_i u_j) - \frac{\partial P}{\partial x_i} + \frac{\partial A_{ij}}{\partial x_j} \tag{2}$$

$$\frac{\partial \rho E}{\partial t} = \frac{\partial (\rho E + P)}{\partial x_i} u_i + \frac{\partial u_j \tau_{ij}}{\partial x_i} + u_i \epsilon_{ijk} J_j B_k + \frac{\partial}{\partial x_k}(\kappa \frac{\partial T}{\partial x_k}) \tag{3}$$

$$\frac{\partial B_i}{\partial t} = \epsilon_{ijk} \frac{\partial}{\partial x_j}(\epsilon_{klm} u_l B_m) + \lambda \frac{\partial^2 B_i}{\partial x_k^2} \tag{4}$$

In the induction equation(4) , λ is the magnetic diffusivity ($\lambda = (\sigma \mu_b)^{-1}$), and in the momentum equation(2), A_{ij} is MHD shear stress defined by $A_{ij} = \tau_{ij} + T_{ij}$. Here, τ_{ij} is the visous tensor and T_{ij} is the defined as $\epsilon_{ijk} J_j B_k = \partial T_{ij}/\partial x_j = \partial[(B_i B_j/\mu_b) - (\mathbf{B}^2/2\mu_b)\delta_{ij}]/\partial x_j$. The first term of T_{ij} is like the viscous stress, and the second one is the magnetic pressure term. In the energy equation, κ is the thermal conductivity and $E = e + \frac{1}{2} u_k u_k$ is the total energy of the fluid per unit mass.

By applying a spatial filter (Favre averaging) to the above equations,[15] the flow variables can be decomposed into the resolved and the unresolved parts, and then the LES governing equations are obtained. The spatial filter is based on the local grid width $\overline{\Delta}$, which is defined by $\widetilde{f} = \overline{\rho f}/\bar{\rho}$ where $\bar{\star}$ means spatial averaging. The resulting filtered equations are:

$$\frac{\partial \bar{\rho}}{\partial t} = -\frac{\partial}{\partial x_j}(\bar{\rho} \tilde{u}_j) \tag{5}$$

$$\frac{\partial \bar{\rho} \tilde{u}_i}{\partial t} = -\frac{\partial}{\partial x_j}(\bar{\rho} \tilde{u}_i \tilde{u}_j - \bar{a}_{ij} + \tau_{ij}^{sgs,v}) - \frac{\partial \bar{P}}{\partial x_i} \tag{6}$$

$$\frac{\partial \bar{\rho} \tilde{E}}{\partial t} = -\frac{\partial}{\partial x_i}\left[\left(\bar{\rho}\tilde{E} + \bar{P}\right)\tilde{u_i} + \bar{q}_i - \tilde{u_j}\bar{a}_{ij} - H_i^{sgs} - \sigma_i^{sgs,v} - q_i^{sgs}\right] \tag{7}$$

$$\frac{\partial \bar{B}_i}{\partial t} = -\frac{\partial}{\partial x_j}(\tilde{u}_j \bar{B}_i - \bar{B}_j \tilde{u}_i + \tau_{ij}^{sgs,b}) + \lambda \frac{\partial^2 \bar{B}_i}{\partial x_k^2} \tag{8}$$

Here, $\bar{q}_i$ is the filtered heat flux given by $\bar{q}_i = \bar{\kappa}\partial\tilde{T}\partial x_j + q_i^{sgs}$ and $\bar{a}_{ij}$ is the resolved part of A_{ij}. The subgrid terms that require closure are: thesubgrid shear stress: $\tau_{ij}^{sgs,v} = -(\tau_{ij}^{sgs,v,v} - \tau_{ij}^{sgs,v,a})$ where $\tau_{ij}^{sgs,v,v} = (\bar{\rho}\widetilde{u_i u_j} - \bar{\rho}\tilde{u}_i\tilde{u}_j)$ is the conventional (flow) subgrid Reynolds stress, and $\tau_{ij}^{sgs,v,a} = (\tilde{A}_{ij} - \bar{a}_{ij})$ is the magnetic subgrid stress. The subgrid heat flux: $H_i^{sgs,v} = (\bar{\rho}\widetilde{Eu_i} - \bar{\rho}\tilde{E}\tilde{u}_i) + \overline{Pu_i} - \bar{P}\tilde{u}_i)$, the subgrid viscous work: $\sigma_i^{sgs,v} = \widetilde{u_i A_{ij}} - \tilde{u}_i\bar{a_{ij}}$, the subgrid thermal conductive flux: $\bar{q}_i^{sgs} = \bar{\kappa}\overline{\frac{\partial T}{\partial x_i}} - \bar{\kappa}\frac{\partial\bar{T}}{\partial x_i}$, and ther subgrid magnetic flux: $\tau_{ij}^{sgs,b} \approx (\widetilde{\tilde{u}_i B_j} - \tilde{u}_i\bar{B}_j) - (\overline{B_i\tilde{u}_j} - \bar{B}_i\tilde{u}_j)$.

In the above equation, $\bar{a}_{ij}$ is the resolved part of A_{ij}. The closure of the $\tau_{ij}^{sgs,b}$ term is one of the primary challenges in the MHD turbulence model. The fluctuating component of the magnetic field in $\tau_{ij}^{sgs,v,a}$ is the Reynolds stress. This negative contribution to the eddy viscosity is the dominating effect of the magnetic field. An extension of the Smagorinsky model is proposed by Shimomura.[5] This model simply introduces a negative eddy viscosity to account for the MHD effect. Shimomura closed the model by using a dimensional analysis of the mean magnetic field. in constract, the MHD LDKM model developed in this paper uses *the subgrid kinetic energy* ($k^{sgs} = \frac{1}{2}(\widetilde{u_k u_k} - \tilde{u}_k\tilde{u}_k)$) and *the subgrid magnetic energy* ($k^{sgs,b} = \frac{1}{2\mu_b}(\overline{B_k B_k} - \bar{B}_k\bar{B}_k)$) to close the SGS equations. The total energy (the sum of k^{sgs} and $k^{sgs,b}$) is conserved for ideal MHD turbulence, which means that the viscosity(ν) and λ vanishes (inviscid and no Joule dissipation case). The available energy changes between kinetic and magnetic energy forms at the small scale as well as the large scale.

The LES governing equations for k^{sgs} and $k^{sgs,b}$ are derived, and given below:

$$\frac{\partial\bar{\rho}k^{sgs}}{\partial t} = -\frac{\partial}{\partial x_j}(\bar{\rho}k^{sgs}\tilde{u}_j) - (\overline{\frac{\partial P}{\partial x_j}u_j} - \frac{\partial\bar{P}}{\partial x_i}\tilde{u}_i) + (\widetilde{\frac{\partial A_{ij}}{\partial x_j}}\tilde{u}_i - \frac{\partial\bar{a}_{ij}}{\partial x_j}\tilde{u}_i) - \frac{\partial}{\partial x_j}(\widetilde{\rho k u_j} - \bar{\rho}\tilde{k}\tilde{u}_j) + \frac{\partial\tau_{ij}^{sgs,v}\tilde{u}_i}{\partial x_j} - \tau_{ij}^{sgs,v}\frac{\partial\tilde{u}_i}{\partial x_j} \tag{9}$$

$$\frac{\partial}{\partial t}(k^{sgs,b}) = -\frac{1}{2\mu_b}\left[\overline{\frac{\partial}{\partial x_j}(\tilde{u}_j b'_i - b'_j\tilde{u}_i)\cdot b'_i} + \overline{\frac{\partial}{\partial x_j}(u'_j\bar{B}_i - \bar{B}_j u'_i)\cdot b'_i} + \overline{\frac{\partial\tau_{ij}^{sgs,b'}}{\partial x_j}\cdot b'_i}\right] + \lambda\frac{\partial^2 k^{sgs,b}}{\partial x_k^2} - \frac{\lambda}{2\mu_b}(\overline{\frac{\partial B_j}{\partial x_i}\frac{\partial B_j}{\partial x_i}} - \frac{\partial\bar{B}_j}{\partial x_i}\frac{\partial\bar{B}_j}{\partial x_i}) \tag{10}$$

where u'_i, b'_i is the fluctuation part of velocity and magnetic field is defined as $u'_i = u_i - \tilde{u}_i$, $b'_i = B_i - \bar{B}_i$, respectively. Here k is the kinetic energy ($k = \frac{1}{2}u_k u_k$). In Eq (10), the first three terms on the right-hand side is the subgrid dissipation term as a result of a nonlinear interaction between the velocity field and the magnetic field. The fourth is the subgrid magnetic energy diffusion term, and the last is the subgrid dissipation term. All of these terms except the fourth one require closure.

B. Closure of LES equation

The LES momentum equation contains two subgrid shear stresses that must be modeled: $\tau^{sgs,v,v}$ and $\tau^{sgs,v,a}$. Gradient diffusion subgrid models and dimension analysis techniques are used to close these terms.[3,7] The final forms are:

$$\tau^{sgs,v,v} = -2\bar{\rho}\nu_t^v(\tilde{S}_{ij} - \frac{1}{3}\tilde{S}_{kk}\delta_{ij}) + \frac{2}{3}\bar{\rho}k^{sgs}\delta_{ij} \tag{11}$$

$$\tau^{sgs,v,a} = -2\nu_t^a(\bar{M}_{ij} - \frac{1}{3}\bar{M}_{kk}\delta_{ij}) - \frac{1}{3}k^{sgs,b}\delta_{ij} \tag{12}$$

$$\nu_t^v = C_\nu^{v,v}\sqrt{k^{sgs}}\bar{\triangle} \tag{13}$$

$$\nu_t^a = C_\nu^{v,a}\sqrt{\frac{k^{sgs,b}}{\mu_b}}\bar{\triangle} \tag{14}$$

In Eq(12), $\bar{M}_{ij}$ is the mean magnetic strain tensor given as $\bar{M}_{ij} = (1/2)(\partial\bar{B}_i/\partial x_j + \partial\bar{B}_j/\partial x_i)$, and $C^{v,v}$ and $C^{v,a}$ are model coefficients that are locally determined. Here, $\bar{\triangle} = (\triangle x \triangle y \triangle z)^{1/3}$ is the local filter width. Combining the above equations results in the following equation for k^{sgs}.

$$\frac{\partial\bar{\rho}k^{sgs}}{\partial t} = -\frac{\partial}{\partial x_i}\bar{\rho}k^{sgs}\tilde{u}_i + \frac{\partial}{\partial x_i}\left\{\frac{(\bar{\rho}\nu_e - \sqrt{\mu_b\bar{\rho}}\nu_t^a)}{Pr_t}\frac{\partial k^{sgs}}{\partial x_i}\right\} - \tau_{ij}^{sgs,v}\frac{\partial\tilde{u}_j}{\partial x_i} - \frac{\bar{\rho}C_\epsilon}{\bar{\triangle}}(k^{sgs} + \frac{k^{sgs,b}}{\bar{\rho}})^{\frac{3}{2}} \tag{15}$$

In Eq(15), ν_e $(= \nu_t^v + \nu)$ is the total viscosity. The model coefficients, $C_\nu^{v,v}$, $C_\nu^{v,a}$ and C_ϵ are implicitly coupled and require additional closure. Pr_t is a turbulent Prandtl number that is currently assumed to be unity. The unclosed term in the magnetic induction equation, $\tau^{sgs,b}$ plays a crucial role in sustaining the mean magnetic field. From the location of the fluctuating component of the magnetic field, b_i', in the induction equation, it can be shown that b_i' and $\bar{B}_i$ are linearly related.[16] By this argument, E_T^k $(= \overline{\epsilon_{kij}u_i'b_j'})$, the so-called turbulent electromotive force, is linearly dependent on $\bar{B}_i$ if the initial value of b' is zero. This is called the α-effect. Yoshizawa analyzed this effect using the two-scale direct-interaction approximation(TSDIA)[6] and investigated the relationship between $\tau^{sgs,v}$ and $\tau^{sgs,b}$ through ν_t^v and ν_t^a:

$$\begin{cases} \tau_{ij}^{sgs,b} = -2\epsilon_{kij}E_T^k \\ E_T^k = \alpha\bar{B}_k - \beta\bar{J}_k + \gamma\bar{\Omega}_k \\ \alpha = \alpha^{'}\sqrt{k^{sgs}}, \quad \beta = \frac{5}{7}(\nu_t^v\mu_b), \quad \gamma = \frac{5}{7}(\nu_t^a\mu_b) \end{cases} \tag{16}$$

In above set of equations, $\bar{J}_k$ is the mean current defined by $\epsilon_{kij}\partial x_i/\partial\bar{B}_j$ and $\bar{\Omega}_k$ is the mean vorticity. The two model coefficients β,γ are closed, but $\alpha^{'}$ is not. This new model coefficient will be discussed in the next section. The interpretation of α, β and γ are as follows. The α-effect is critical in MHD turbulence where small scale motion leads to the generation of a poloidal field from an azimuthal field and contributes to a large scale magnetic field. The induced magnetic field is approaching to the configuration of $\epsilon_{kij}\bar{J}_i\bar{B}_j = 0$. The physical meaning of β can be understood easily by noticing that this merges into the diffusion term and enhances the magnetic diffusivity $(\lambda \to \lambda + \beta)$. Finally, γ is related to the cross-helicity effect by the fact that $\vec{\bar{J}}$ is aligned to $\vec{\bar{\Omega}}$. A detailed discussion of each of the mechanisms related to these coefficients are given by Yokoi.[9]

The final modeled magnetic induction equation(4) is expressed as:

$$\frac{\partial\bar{B}_i}{\partial t} = -\frac{\partial}{\partial x_j}(\tilde{u}_j\bar{B}_i - \bar{B}_j\bar{u}_i - 2\epsilon_{kij}E_T^k) + \lambda\frac{\partial^2\bar{B}_i}{\partial x_k^2} \tag{17}$$

$$\tag{18}$$

The first three terms on the right-hand-side of the magnetic energy, Eq (10), is rewritten as a transport term and a production term in order to close these terms by the same technique used in the conventional LDKM modeling. Thus,

$$-[\overline{\frac{\partial}{\partial x_j}(\tilde{u}_j b'_i - b'_j\tilde{u}_i)b_i'} + \overline{\frac{\partial}{\partial x_j}(u'_j\bar{B}_i - \bar{B}_j u'_i)b_i'} + \overline{\frac{\partial\tau_{ij}^{sgs,b'}}{\partial x_j}b_i'}] = -\overline{\frac{\partial\tau_{ij}^{sgs,b'}b_i'}{\partial x_j}} + \overline{\tau_{ij}^{sgs,b'}\frac{\partial b'}{\partial x_j}_i} \tag{19}$$

The first term on the right-hand side of Eq(19) is the transport term and the second is the production term. It is difficult to calculate $\tau^{sgs,b'}$ exactly since it contains the nonlinear product of a fluctuating and a mean value of the velocity and magnetic field. In this paper, the aim is not a reconstruction of the eliminated information, but rather an attempt to model the effects of the subgrid-scale dynamics using a resolved scale. Therefore, by replacing $\tau^{sgs,b'}$ with $\tau^{sgs,b}$ and b'_i with $\bar{B}_i$, it is possible to simplify the modeling of these terms. Finally, the modeled subgrid magnetic energy equation is:

$$\frac{\partial k^{sgs,b}}{\partial t} = -\frac{1}{2\mu_b}\frac{\partial}{\partial x_j}(\tau_{ij}^{sgs,b}\bar{B}_i) + \frac{1}{2\mu_b}\tau_{ij}^{sgs,b}\frac{\partial \bar{B}_i}{\partial x_j} + \lambda\frac{\partial^2 k^{sgs,b}}{\partial x_k^2} - \frac{C_{\epsilon,b}k^{sgs,b}}{\sigma\mu_b\bar{\triangle}^2} \tag{20}$$

$$\tag{21}$$

where $C_{\epsilon,b}$ is a model coefficient.

C. Dynamic calculation of model coefficients

The above equations for MHD turbulence are still not completely closed since there are five model coefficents that still need to be determined: $C_\nu^{v,v}$, $C_\nu^{v,a}$, C_ϵ, $C_{\epsilon,b}$ and $\alpha^{'}$. These values are not pre-determined by experimental/DNS data. Instead, they are computed dynamically. The details of the formulation of the LDKM model can be found elsewhere.[17,18] The critical assumption is that there is similarity between the subgrid and test-filtered dynamics. Therefore, an analogous test field expression can be obtained by performing the test filter operation on the exact form. Hereafter, $\hat{f}$ denotes the test filtering and the test filter level is $\hat{\triangle}$ $(= 2\bar{\triangle})$.

1. *The $\alpha^{'}$ coefficient*

The procedure for computing $\alpha^{'}$ starts with the exact expression for $\tau_{ij}^{sgs,b}$ to the model equation $(\alpha^{'}\sqrt{k^{sgs}}\bar{B}_k - \beta\bar{J}_k + \gamma\bar{\Omega}_k = E_T^k \approx 1/2\epsilon_{kij}((\overline{\tilde{u}_j\bar{B}_i} - \hat{\tilde{u}}_j\hat{\bar{B}}_i) - (\overline{\bar{B}_j\tilde{u}_i} - \hat{\bar{B}}_j\hat{\tilde{u}}_i)))$. If all terms on the right were known, $\alpha^{'}$ could be directly computed. However, in LES, the right hand also remains unknown. On the other hand, to construct an expression similar to the above equation on the test filter grid is possible.

$$\alpha^{'}\sqrt{\hat{k}^{sgs}}\bar{B}_k - \beta\bar{J}_k + \gamma\bar{\Omega}_k = E_T^k \approx \frac{1}{2}\epsilon_{kij}((\widehat{\tilde{u}_j\bar{B}_i} - \hat{\tilde{u}}_j\hat{\bar{B}}_i) - (\widehat{\bar{B}_j\tilde{u}_i} - \hat{\bar{B}}_j\hat{\tilde{u}}_i)) \tag{22}$$

Here, $\hat{k}^{sgs}$ is the subgrid kinetic energy at the test filter level as $\hat{k}^{sgs} = \frac{1}{2}[\widehat{\bar{\rho}\tilde{u}_k^2}/\hat{\bar{\rho}} - \widehat{\bar{\rho}\tilde{u}_k}^2/\hat{\bar{\rho}}^2]$. In the above equation, all terms expect $\alpha^{'}$ are known, and $\alpha^{'}$ can be easily extracted by algebraic rearrangement. However, the condition is over-specified (*i.e.,* 3 equations, one unknown). Based on the similar idea proposed by Lilly,[19] the model error Er^k is defined by

$$Er^k = L^k - \alpha^{'}\sqrt{\hat{k}^{sgs}}\bar{B}_k \tag{23}$$

where $L^k = 1/2\epsilon_{kij}((\widehat{\tilde{u}_j\bar{B}_i} - \hat{\tilde{u}}_j\hat{\bar{B}}_i) - (\widehat{\bar{B}_j\tilde{u}_i} - \hat{\bar{B}}_j\hat{\tilde{u}}_i)) + \beta\bar{J}_k - \gamma\bar{\Omega}$. Er^k could be positive or negative number, therefore minimizing the RMS of the error. The derivative with respect to the model coefficient should be zero.

$$\frac{\partial Er^k Er^k}{\partial\alpha^{'}} = 0 = -2\sqrt{\hat{k}^{sgs}}L_k\bar{B}_k + 2\alpha^{'}\hat{k}^{sgs}\bar{B}_k\bar{B}_k \tag{24}$$

From this, $\alpha^{'}$ can be computed :

$$\alpha^{'} = -\frac{L_k\bar{B}_k}{\sqrt{\hat{k}^{sgs}}\bar{B}_k\bar{B}_k} \tag{25}$$

It can be seen that $\alpha^{'}$ has a weak dependence on the magnetic field and is a property of the turbulence. E_T^k becomes zero when there are no partial alignment of the small-scale eddies, since the cumulative influence of many small-scale activity can give rise to a large-scale magnetic field. Therefore, modeling $\alpha^{'}$ has to consider such a character, and it has been pointed out that there is a relationship between the turbulent helicity and α.[6] Establishing this relationship requires additional closures for these terms and increases the number of model coefficients. In this model, L_k has a information of small-scale motion and enables the model to imitate this physical significance of α. The evaluation of $\alpha^{'}$ using Eq (25) is also stable since the denominator is well defined and non-zero in the flow field.

2. The dissipation model coefficient, C_ϵ

The expression of C_ϵ for the non-MHD compressible case is derived by Kim and Menon.[18] In the MHD case, additional dissipation terms appear: $\epsilon^b = \widetilde{u_i \partial T_{ij}}/\partial x_j - \tilde{u}_i \partial \bar{T}_{ij}/\partial x_j$. Therefore, the sum of the conventional dissipation (ϵ^v) and ϵ^b can be thought of as the total MHD compressible dissipation:

$$\begin{aligned}\epsilon \approx \epsilon^v + \epsilon^b = \hat{\mu}\left\{\widehat{\frac{\partial \tilde{u}_j}{\partial x_i}}\frac{\partial \tilde{u}_j}{\partial x_i} - \frac{\partial}{\partial x_i}\left(\frac{\widehat{\bar{\rho}\tilde{u}_j}}{\hat{\bar{\rho}}}\right)\frac{\partial}{\partial x_i}\left(\frac{\widehat{\bar{\rho}\tilde{u}_j}}{\hat{\bar{\rho}}}\right)\right\} + \tilde{u}_i\widehat{\frac{\partial \bar{T}_{ij}}{\partial x_j}} - \frac{\widehat{\bar{\rho}\tilde{u}_j}}{\hat{\bar{\rho}}}\frac{\partial \bar{T}_{ij}}{\partial x_j} \\ \approx \frac{\hat{\bar{\rho}} C_\epsilon}{\hat{\triangle}}\left(\hat{k}^{sgs} + \frac{\hat{k}^{sgs,b}}{\hat{\bar{\rho}}}\right)^{\frac{3}{2}}\end{aligned} \tag{26}$$

Here $\hat{k}^{sgs,b}$ is the subgrid magnetic energy at the test filter level ($\hat{k}^{sgs,b} = \frac{1}{2\mu_b}[\widehat{\bar{B}_k\bar{B}_k} - \hat{\bar{B}}_k\hat{\bar{B}}_k]$). Finally, the modeled expression for C_ϵ can be obtained using an earlier defined approach:[18]

$$C_\epsilon = \frac{\left\{\hat{\mu}\left\{\widehat{\frac{\partial \tilde{u}_j}{\partial x_i}}\frac{\partial \tilde{u}_j}{\partial x_i} - \frac{\partial}{\partial x_i}\left(\frac{\widehat{\bar{\rho}\tilde{u}_j}}{\hat{\bar{\rho}}}\right)\frac{\partial}{\partial x_i}\left(\frac{\widehat{\bar{\rho}\tilde{u}_j}}{\hat{\bar{\rho}}}\right)\right\} + \tilde{u}_i\widehat{\frac{\partial \bar{T}_{ij}}{\partial x_j}} - \frac{\widehat{\bar{\rho}\tilde{u}_j}}{\hat{\bar{\rho}}}\frac{\partial \bar{T}_{ij}}{\partial x_j}\right\}\hat{\triangle}}{\hat{\bar{\rho}}\left(\hat{k}^{sgs} + \frac{\hat{k}^{sgs,b}}{\hat{\bar{\rho}}}\right)^{\frac{3}{2}}} \tag{27}$$

3. The MHD dissipation model coefficient, $C_{\epsilon,b}$

By assuming scale similarity mentioned above, one can estimate the test field dissipation as follows:

$$\frac{\lambda}{2\mu_b}\left(\widehat{\frac{\partial \bar{B}_j}{\partial x_i}}\frac{\partial \bar{B}_j}{\partial x_i} - \frac{\partial \hat{\bar{B}}_j}{\partial x_i}\frac{\partial \hat{\bar{B}}_j}{\partial x_i}\right) \approx \frac{C_{\epsilon,b}\hat{k}^{sgs,b}}{\sigma\mu_b\hat{\triangle}^2} \tag{28}$$

Except for the model coeffient, $C_{\epsilon,b}$, all terms are already specified. Therefore, an expression for $C_{\epsilon,b}$ can be easily computed as:

$$C_{\epsilon,b} = \frac{\hat{\triangle}^2}{2\hat{k}^{sgs,b}\mu_b}\left(\widehat{\frac{\partial \bar{B}_j}{\partial x_i}}\frac{\partial \bar{B}_j}{\partial x_i} - \frac{\partial \hat{\bar{B}}_j}{\partial x_i}\frac{\partial \hat{\bar{B}}_j}{\partial x_i}\right) \tag{29}$$

4. The MHD subgrid stress model coefficient, $C_\nu^{v,a}$

The same procedure is used for computing $C_\nu^{v,a}$. An analogous test field expression is written as:

$$\hat{\bar{T}}_{ij} - \hat{\tilde{t}}_{ij} + \frac{1}{3}\hat{k}^{sgs,b}\delta_{ij} \approx -2C_\nu^{v,a}\sqrt{\frac{\hat{k}^{sgs,b}}{\mu_b}}\hat{\triangle}\left(\hat{\bar{M}}_{ij} - \frac{1}{3}\hat{\bar{M}}_{kk}\delta_{ij}\right) \tag{30}$$

where $\hat{\bar{T}}_{ij}$ is defined by $(\widehat{\bar{B}_i\bar{B}_j}/\mu_b) - (\widehat{\bar{B}_k\bar{B}_k}/2\mu_b)\delta_{ij}$, and $\hat{\tilde{t}}_{ij}$ is defined by $(\hat{\bar{B}}_i\hat{\bar{B}}_j/\mu_b) - (\hat{\bar{B}}_k\hat{\bar{B}}_k/2\mu_b)\delta_{ij}$. The value of $C_\nu^{v,a}$ is determined by the least-square method. The result is as:

$$C_\nu^{v,a} = -\frac{L_{ij}^b D_{ij}^b}{2D_{ij}^b D_{ij}^b} \tag{31}$$

where, $L_{ij}^b = \hat{\bar{T}}_{ij} - \hat{\tilde{t}}_{ij} + \frac{1}{3}\hat{k}^{sgs,b}\delta_{ij}$ and, $D_{ij}^b = \sqrt{\frac{\hat{k}^{sgs,b}}{\mu_b}}\hat{\triangle}\left(\hat{\bar{M}}_{ij} - \frac{1}{3}\hat{\bar{M}}_{kk}\delta_{ij}\right)$.

5. The subgrid stress model coefficient, $C_\nu^{v,v}$

No modification is needed since the MHD effect is only related to $C_\nu^{v,a}$. The expression of $C_\nu^{v,v}$ is derived by Kim and Menon:[18]

$$C_\nu^{v,v} = -\frac{L_{ij}D_{ij}}{2D_{ij}D_{ij}} \tag{32}$$

where, $L_{ij} = \bar{\rho}\widehat{\tilde{u}_i\tilde{u}_j} - \frac{\widehat{\bar{\rho}\tilde{u}_j}\widehat{\bar{\rho}\tilde{u}_j}}{\hat{\bar{\rho}}} - \frac{1}{3}\left\{\bar{\rho}\widehat{\tilde{u}_k\tilde{u}_k} - \frac{\widehat{\bar{\rho}\tilde{u}_k}\widehat{\bar{\rho}\tilde{u}_k}}{\bar{\rho}}\right\}\delta_{ij}$ and, $D_{ij} = 2C_\nu^{v,v}\hat{\triangle}\hat{\bar{\rho}}\hat{k}^{sgs}\left\{\hat{\tilde{S}}_{ij} - \frac{1}{3}\hat{\tilde{S}}_{kk}\delta_{ij}\right\}$.

Other subgrid terms appear in the LES filtered energy have to be closed. The subgrid total enthalpy flux H_i^{sgs} is also modeled using the eddy viscosity and a gradient assumption as:

$$H_i^{sgs} \approx -\frac{(\bar{\rho}\nu_e - \sqrt{\mu_b\bar{\rho}}\nu_t^a)}{Pr_t}\frac{\partial\tilde{H}}{\partial x_i} \tag{33}$$

σ_i^{sgs} is often neglected in conventional LES approaches.[20] However, this still remains uncertain for MHD flow.

III. $\partial B_i/\partial x_i = 0$ constraint

In the previous section, we formulated the closed LES equations to solve MHD turbulence under the condition $\partial B_i/\partial x_i = 0$. These equations are valid from the theoretical viewpoint. However, from the numerical viewpoint, this is not always true, especially when using finite-difference or finite-volume codes with limited numerical accucuracy. Ideally, $\partial B_i/\partial x_i$ converges to zero as the grid resolution $\triangle X$ and $\triangle t$ approach zero. Unfortunately, this negates the purpose of LES and increases computational time unnecessarily. Thus, a numerical scheme is necessary to force the $\partial B_i/\partial x_i$ to become zero or at least a small enough (acceptable) value. A conmprehensive discussion is given by Gabor.[21] In this paper, several schemes are evaluated, such as *the eight-wave formulation*[22] that enforces the truncation error to be zero, *the projection scheme*[23] that enforces the constraint in some discretization by projection of the magnetic field and *the constrained transport scheme*[24] that conserves $\partial B_i/\partial x_i$ to machine accuracy in some discretization for every grid cell. At present, *the projection scheme* is used, partly based on a best compromise between accuracy and computational cost.

A. The projection scheme

In *the projection scheme* proposed by Brackbill and Barnes,[23] the vector field B_k is decomposed into the two parts: a curl and a gradient so that: $B_k = \epsilon_{kij}\partial A_i/\partial x_j + \partial\phi/\partial x_k$. Here A is the vector potential and has a physical meaning like a streamline. The variable ϕ does not have any significant meaning. A nonzero of ϕ results from numerical error. Taking the divergence of the above equation, a Poisson equation is obtained: $\partial^2\phi/\partial {x_k}^2 = \epsilon_{kij}\partial B_i/\partial\bar{x}_j$

If we successfully solve this equation for ϕ, we can modify B such that we calculate numerically $B_i^{'} = B_i - \partial\phi/\partial x_i$ If the Poisson equation can be accurately solved, $\partial B_i^{'}/\partial x_i$ must be zero. In practice, $\partial B_i^{'}/\partial x_i$ is not zero, but much less than $\partial B_i/\partial x_i$. In order to achieve the criteria of accuracy, we need to iterate this operation. In many respects, this requirement is similar to the $\partial u_i/\partial x_i = 0$ requirement in incompressible flow.

B. $\partial B_i/\partial x_i$ reduction

In Figure 1, the history of $\partial\bar{B}_i/\partial x_i$, $\partial\tilde{u}_i/\partial x_i$, kinetic energy and magnetic energy are shown for two cases; without modification and with modification. At t = 0.01, the magnetic field is initiated. Without modification, the magnitude of $\partial\bar{B}_i/\partial x_i$ is about 5 times larger than the $\partial\tilde{u}_i/\partial x_i$. The initial increase of $\partial\bar{B}_i/\partial x_i$ is caused by the incorrect initialization of magnetic field. The slow decrease is related to the reduction of magnetic turbulence, therefore, the relative importance of a nonzero effect on the numerical result is significant. On the other hand, with modification, $\partial\bar{B}_i/\partial x_i$ become about one fifth of $\partial\tilde{u}_i/\partial x_i$ and does not have an initial peak. This means that *the projection scheme* successfully eliminates the unphysical part of the magnetic field and keeps $\partial\bar{B}_i/\partial x_i$ relatively small. The unphysical non-zero effect can be seen in the

gradient of kinetic energy and magnetic energy variation with time. The case without modification has a steeper in kinetic energy, but is slightly less steep in the magnetic field. This can be explained by considering the magnetic and kinetic energy equations in which the unphysical non-zero effect is considered. In Eq (34), the additional term that disappears under the condition $\partial B_i/\partial x_i = 0$ appears:

$$\frac{\partial \bar{\rho}\bar{k}^*}{\partial t} = -\frac{\partial}{\partial x_j}(\bar{\rho}\bar{k}^*\tilde{u}_j) - \frac{\partial \bar{P}}{\partial x_i}\tilde{u}_i + \frac{\partial \bar{a}_{ij}}{\partial x_j}\tilde{u}_i + \frac{\partial \tau_{ij}^{sgs,v}}{\partial x_j}\tilde{u}_i - \frac{\bar{B}_i\tilde{u}_i}{\mu_b}\frac{\partial \bar{B}_j}{\partial x_j} \tag{34}$$

where $\bar{k}^*$ is the resolved kinetic energ defined by $\bar{k}^* = \frac{1}{2}\tilde{u}_i\tilde{u}_i$. The counterpart of this term also appears in magnetic energy equation:

$$\frac{\partial}{\partial t}(\bar{k}^{*,b}) = - \bigtriangledown_j (\tilde{u}_j\bar{B}_i - \bar{B}_j\tilde{u}_i + \tau_{ij}^{sgs,b})\frac{\bar{B}_i}{2\mu_b} + \lambda\frac{\partial^2 \bar{B}_i}{\partial x_k^2}\frac{\bar{B}_i}{2\mu_b} + \frac{\bar{B}_i\tilde{u}_i}{2\mu_b}\frac{\partial \bar{B}_j}{\partial x_j} \tag{35}$$

where $\bar{k}^{*,b}$ is the resolved magnetic energy defined by $\bar{k}^{*,b} = \frac{\bar{B}_i\bar{B}_i}{2\mu_b}$. It shows that the unphysical non-zero effect plays an additional role in transfering the energy between the magnetic energy and kinetic energy. Moreover, this effect is acceleration of the plasma parallel to the field lines because $\frac{\bar{B}_i}{\mu_b}\partial\bar{B}_k/\partial x_k$ has to be added in Lorentz force term.

IV. Numerical Results

To test the validity of the MHD LDKM derived in the above section, two types of simulations were conducted. In the first case the effect of an externally applied magnetic field on an initially isotropic MHD turbulent flow is investigated. In the second case, homogeneous MHD turbulence is initially introduced in the computational domain so that turbulent decay can be investigated. No external field or forces are applied. Validation of this model is performed qualitatively and quantatively.The numerical solver is an explicit time-integration, finite-volume method that is norminally second-order accurate in space and time.

A. Anisotropic MHD turbulence with external magnetic field

The initial set up for isotropic turbulence is (*case 0* : $R_\lambda = 24, \lambda = \nu = 0.001, L_{box} = 1.5m$ and integral length-scale $= 0.4m$). The grid resolution is 50^3. In Figure 2, the contours of the kinetic energy at different time steps are plotted. Note since the turbulence is rapidly decaying, and therefore, the colormap is rescaled at each time step. An external magnetic field is applied from the bottom to the upper surface. These plots show that the diffusion of angular momentum along the field lines cause the vortex to elongate into a cylindrical shape. It is seen that the small scale turbulent structure is significantly damped by MHD effect. These results qualitatively agree with previous observations of the effect of megnetic field obtained by Knaepen.[4] In his model, the dynamic Smagorinsky model was used, and low magnetic Reynolds number was assumed.

B. Homogeneous MHD turbulence

Freely decaying MHD turbulence simulation is performed. In the initial state, we introduced isotropic turbulent flow field same as *case 0*, and randomly chosed magnetic field. In this case, the averaged magnetic field is zero, and induced magnetic fields are strongly coupled with the flow motion. Because of this interaction, the magnetic energy is temporarily amplified and starts to decay gradually. Compared with the isotropic turbulent case without MHD effect, relatively fast kinetic energy decay was observed (See Figure 3). This is so-called magnetic damping. Motion across magnetic field lines induces a current, causing Joule dissipation. Through this mechanism, the kinetic energy is converted into corresponding amount of thermal energy.

Figure 4 shows the time evolution of the normalized kinetic energy and dissipation. Both spectra roughtly follow a $k^{-5/3}$ and $k^{1/3}$ law. The detail discussion of scaling laws for isotropic MHD turbulence is given by Biskamp[25] and these results are in good agreement. Figure 5 shows the time histories of the spacially averaged α, $C_{\epsilon,b}$ and $C_\nu^{v,a}$, respectively. These rates reach $\alpha \approx 10^{-4}$, $C_{\epsilon,b} \approx 0.5$, and $C_\nu^{v,a} \approx 0.056$ in the flow. For further validation, we compare DNS(128^3) and LES(64^3) results for *case 0*.

In Figures 6 and 7, we plot, respectively the contours of the components of the velocity field and magnetic field at $t = 0.7855$ for DNS and $t = 0.7794$ for LES. Even though there are some discrepancies of the

magnitude, it can be seen that the LES can reproduce the DNS structure well, and the large-scale motions in DNS and LES calculation have common feature.

For the higher level test to examine the detail structure of turbulence, it is required to check the spectral distribution of kinetic energy and dissipation rate. Since turbulence is well characterrized by the distribution of spacial scale of eddies, the agreement of these spectrum data from DNS is critical for LES model. For DNS, the grid size is comparable to dissipation scale-length, on the other hand, LES has the grid spacing that is the in inertial range. Therefore, the modeling of small scale related to the dissipation is a main task of LES. To that end, the slope of the energy and the dissipation rate spectra in the inertial range is a good benchmark since this slope is strongly related to the dissipation mechanizm in small scale.

Figure 8 shows DNS/LES numerical results of the Kolmogorov scaled energy spectrum and dissipation rate spectrum. For the both cases, overall agreement is good. For another validation, we check the time variation of the energy ratio $\Gamma = E^k/E^m$, E^t, and H_m. Biskamp points out that Γ decays in 3D where it is constant in 2D. Also, he found out that the ratio $\Gamma H_m/(E^t)$ remains constant.[25] It can be seen after the MHD turbulence is fully developped ($t \geq 0.22$) in Figure 9 thus our results are consistent with Biskamp's results. This confirms that this current simulation is performing as expected.

Table 1. Initial Condition

	$\mathbf{R_\lambda}$	**Viscosity**	$\mathbf{E^k/E^m}$	$\mathbf{H_m/E^t}$	$\mathbf{H_c/E_t}$
case.1	51	$1.0E-3$	1.0	$\approx 10^{-2}$	$\approx 10^{-2}$
case.2	51	$1.0E-3$	1.0	$\approx 10^{-2}$	$\approx 10^{-0}$

Figure 10 shows the long-time behavior of total energy and energy ratio of E^k to E^m for cases 1 and 2 (see Table1). For case 1, H^c and H^m are set very small. In this case, no back-scatter of magnetic and kinetic energy occurs and the energy transfer from the large-scale eddies to small-scale eddies is smoothly carried out. In constract, case 2 has finite H^c and back-scatter of kinetic energy is expected. Figure 10(a) shows E^t follows the asymptotic decay law for both cases, however, the decaying rate is different. Without back-scatter, case 1 has steeper gradient($E^t \sim t^{-1}$) compared to case 2 ($E^t \sim t^{-2/3}$). Biskamp derived $E^t \sim t^{-2/3}$ theoretically by assuming that H^m was considered invariant during energy decay.[25] However, this assumption is not always satisfied in 3D MHD turbulence. Also, his calculation shows $E^t \sim t^{-1}$ for small H^m. Even though Biskamp attributes these different decay rates to the difference of initial H^m, our calculation shows H^c also plays a significant role in energy decay. The back-scatter of kinetic energy for case 2 can be seen in Figure 10(b). Compared to the case 1, case 2 has relatively large amount of kinetic energy remaining during energy decay.

V. Conclusion

In this paper, a new dynamic subgrid model for LES of compressible MHD turbulence is developed and demonstrated. The five model coefficients are computed dynamically. The major assumption in this closure procedure is that the subgrid dynamics at the grid cutoff scale are similar to the smallest resolved scale (test-scale). It is difficult to simulate MHD turbulence effects because of nonlinear coupling between velocity and magnetic field. For example, the simple expression of $\tau_{ij}^{sgs,b}$ cannot be derived without assuming isotropic and homogeneous turbulence. However, LDKM successfully overcomes these difficulties by using a few realistic assumptions, while removing the necessities of *ad hoc* procedures. To determine the performance of this model, several simulations were carried out. The detail structure of MHD turbulence was examined by comparison of energy and dissipation spectra. Also, time variation of ideal invariants was also investigated. Both tests show that this new model is capable of capturing the MHD turbulence well. Since there is no requirment of low magnetic Reynolds number to simplify the formulation of this model, this can be adapted to a wide variety of physical problems.

VI. Acknowledgment

This research is supported by NASA/GRC through the University Research Engineering and technology institute for Aeropropulsion and Power, under Grant Cooperative Agreement Number NCC3-982.

References

[1]A.V.Gruzinov and P.H.Diamond, "Self-consistent mean field electrodynamics of turbulent dynamos," *Physics of plasmas*, Vol. 2, 1995.

[2]Zhou, Y. and W.H.Matthaeus, "Phenomenology treatment of magnetohydrodynamic turbulence with nonequipartition and anisotropy," *Physics of plasmas*, Vol. 12, 2005.

[3]ü ller, W. and D.Carati, "Dynamic gradient-diffusion subgrid models for incompressible magnetohydrodynamics turbulence," *Physics of Plasma*, Vol. 9, 2002.

[4]B.Knaepen and P.Moin, "Large-eddy simulation of conductive flows at low magnetic Reynolds number," *Center for Turbulence Reserach Annual Reserach Briefs*, 2003.

[5]Shimomura, Y., "Large eddy simulation of magnetohydrodynamics turbulent channel flows under a uniform magnetic field," *Physics of fluids*, 1991.

[6]A.Yoshizawa, "Self-consistent turbulent dynamo modeling of reversed field pinches and planetary magnetic fields," *Physics of plasmas*, 1990.

[7]A.Yoshizawa and .Yokoi, N., "Stationary Large-scale magnetic field generated by turbulent motion in a spherical region," *Physics of plasmas*, Vol. 3, 1996.

[8]N.Seehafer, "nature of the α effect in magnetohydrodynamics," *Physical review E*, Vol. 53, 1996.

[9]Yokoi, N., "Magnetic-field generation and turbulence suppression due to cross-helicity effects," *Physics of Fluids*, Vol. 11, 1999.

[10]U.Frisch, A.Pouquet, J. and A.Mazure, "Relaxation processes in a low-order three -dimensional magnetohydrodynamics model," *Journal of Fluid Mechanics*, Vol. 68, 1975.

[11]Stribling, T. and H.matthaeus, W., "Relaxation processes in a low-order three -dimensional magnetohydrodynamics model," *Physics of Fluids*, 1991.

[12]D.Montgomery, L. and Vahala, G., "Three-dimensional magnetohydrodynamics turbulence in cylindrical geometry," *Physics of fluids*, Vol. 21, 1978.

[13]W.H.Matthaeus, M. and D.C.Montgomery, "turbulent generation of Outward-Traveling Interplanetary Alfvenic Fluctuations," *Physical Review Letters*, Vol. 51, 1983.

[14]S.Liu, C. and J.Katz, "On the properties of similarity subgrid scale models as deduced from measurements in a turbulent jet," *Journal of Fluid Mechanics*, Vol. 275, 1994.

[15]G.Erlebacher, M.Y.Hussaini, C. S. and T.A.Zang, "Toward the large-eddy simulation of compressibleturbulent flows," *Journal of Fluid Mechanics*, Vol. 238, 1992.

[16]P.A.Davidson, "An introduction to magnetohydrodynamics," *Cambridge University Press*, 2001.

[17]Kim, W.-W. and S.Menon, "An unsteady incompressible navier-Stokes solver for Large-Eddy Simulation of turbulent flows," *International Journal for Numerical methods in Fluids*, Vol. 31, 1999.

[18]W.-W. Kim, S. and Mongia, H., "Large-Eddy Simulation of a gas turbine combustor flow," *Combustion Science and technology*, Vol. 143, 1999.

[19]D.K.Lilly, "A proposed modification of the Germano subgrid-scale closure method," *Physics of Fluids*, 1992.

[20]C.Fureby and S-I.Müller, "Large-eddy simulation of reacting flows applied to bluff body stabilized flames," *AIAA journal*, Vol. 33, 1995.

[21]Toth, G., "The $\bigtriangledown \cdot B = 0$ constraint in shock-Capturing magnetohydrodynamic code," *Journal of Computational Physics*, Vol. 161, 2000.

[22]K.G.Powell, "Large-eddy simulation of reacting flows applied to bluff body stabilized flames," *AIAA journal*, 1994.

[23]Brackbill, J. and D.C.Barnes, "The effect of nonzero $\bigtriangledown \cdot B = 0$ on the numerical solution of the magnetohydrodynamic equations," *Journal of Computational Physics*, Vol. 35, 1980.

[24]C.R.Evans and J.F.Hawley, "Simulation of magnetohydrodynamic flows: A constrained transport method," *Astrophyical journal*, 1988.

[25]D.Biskamp and Muller, W.-C., "Scaling properties of three-dimensional isotropic magnetohydrodynamic turbulence," *Physics of plasmas*, Vol. 7, 2000.

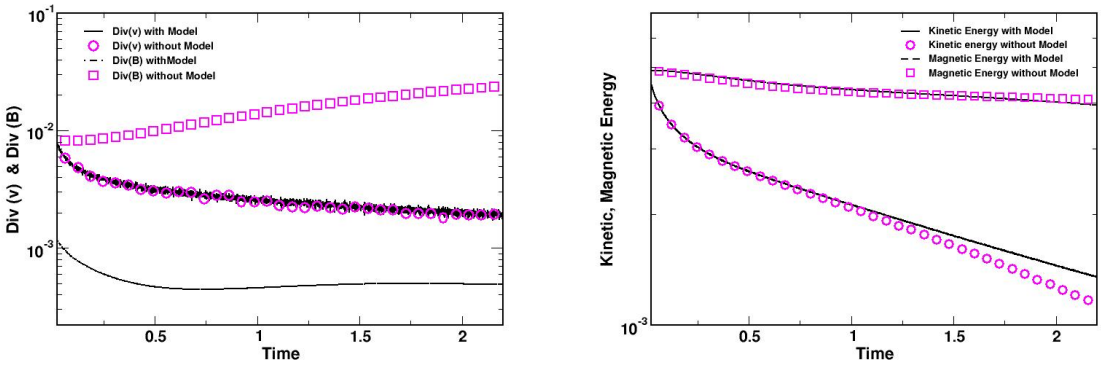

(a) (b)

Figure 1. History of $\vec{\nabla} \cdot \vec{V}$ (a), $\vec{\nabla} \cdot \vec{B}$ (a) kinetic energy (b) and magnetic energy (b) for the case with correction and without correction

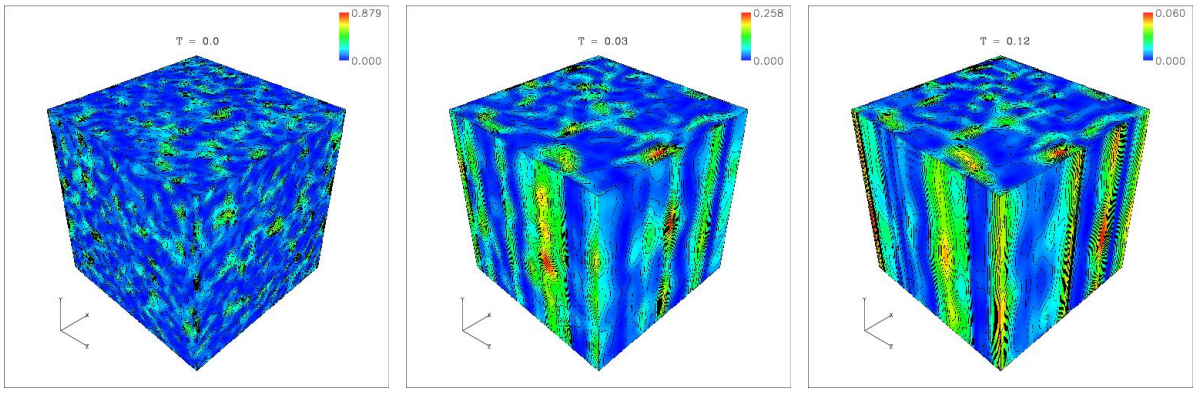

(a) (b) (c)

Figure 2. Contours of the kinetic energy obtained from the MHD LDKM. The times at which the contours are obtained are shown above the figures.

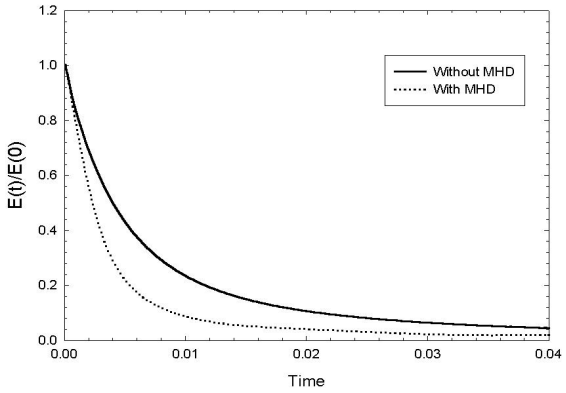

(a)

Figure 3. The time evolution of the kinetic energy

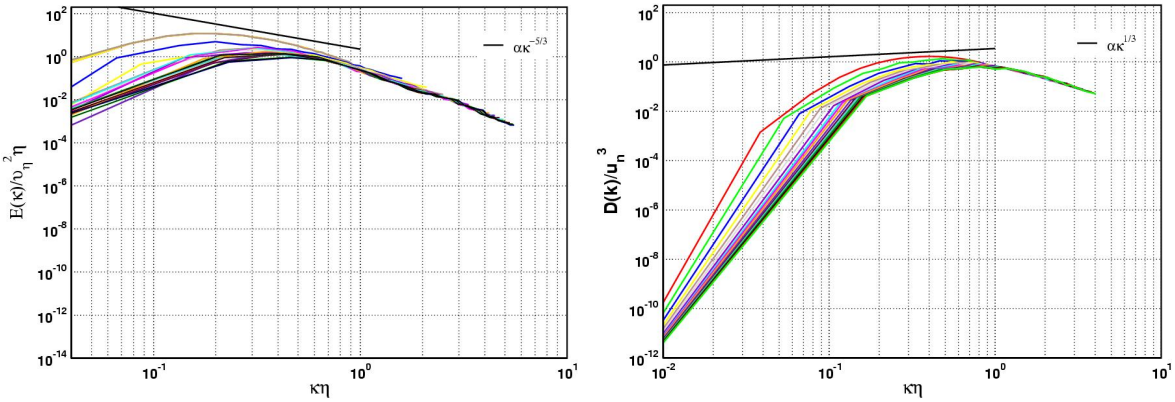

(a) (b)

Figure 4. The time evolution of the normalized energy and dissipation rate spectra

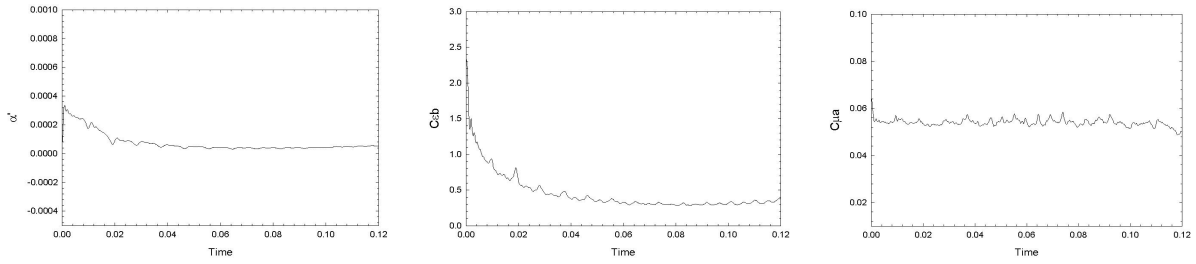

(a) (b) (c)

Figure 5. Time history of the model coefficents (α, $C_{\epsilon,b}$ and $C_{\nu}^{v,a}$) for isotropic turbulence case

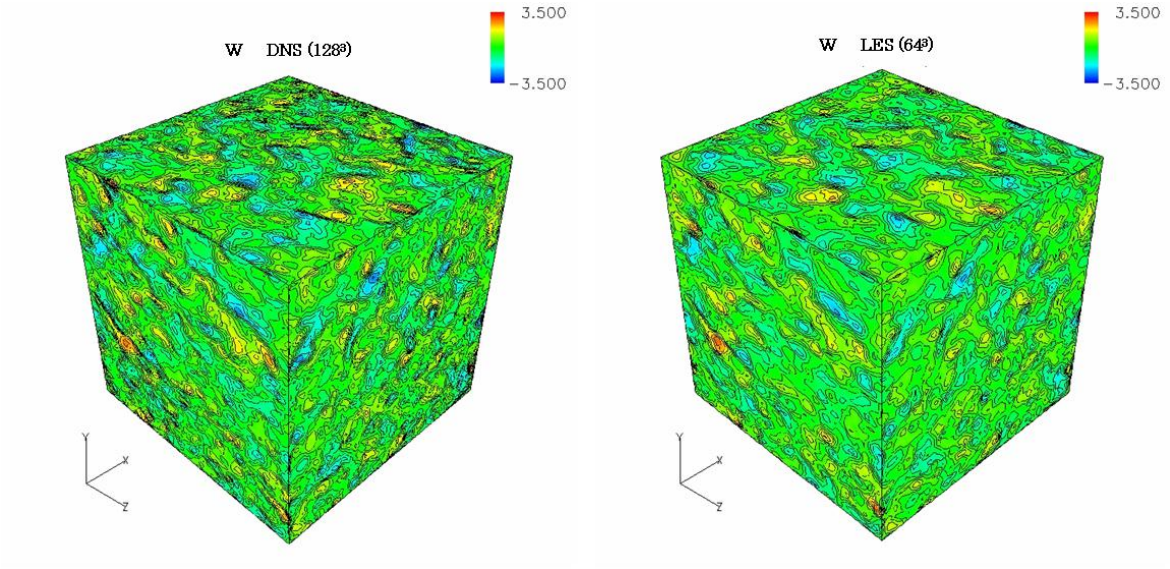

(a) (b)

Figure 6. Comparision of DNS and LES results for snapshot of velocity field profile

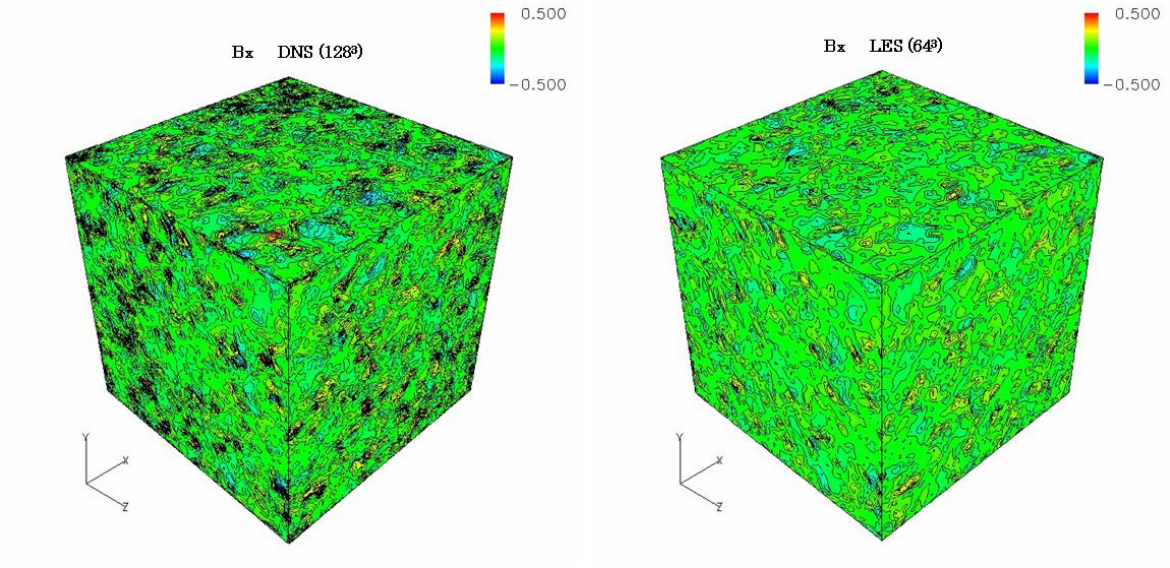

(a) (b)

Figure 7. Comparision of DNS and LES results for snapshot of magnetic field profile

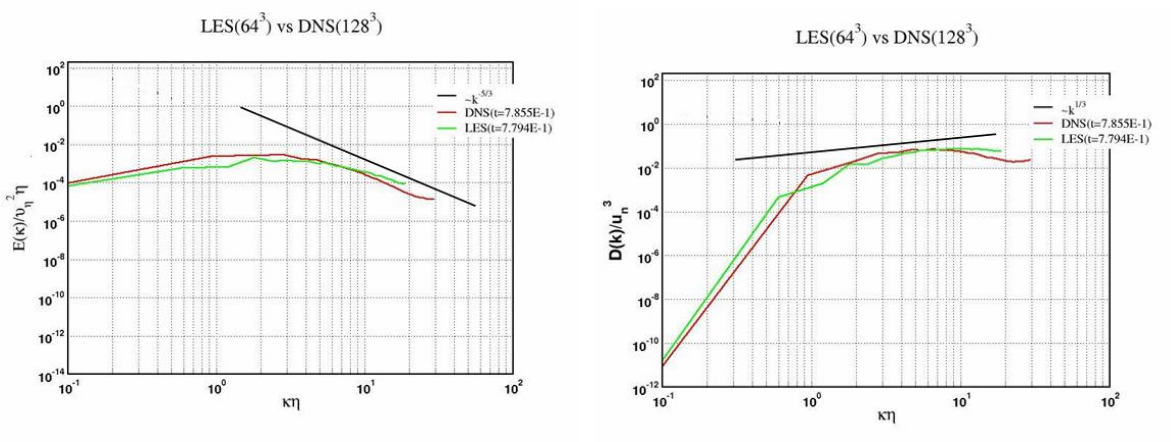

(a) (b)

Figure 8. Comparision of DNS and LES results for energy and dissipation rate spectra

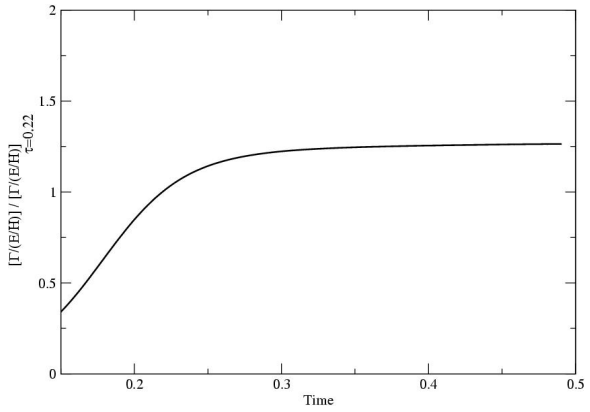

(a)

Figure 9. Time history of $\Gamma/(E/H)$

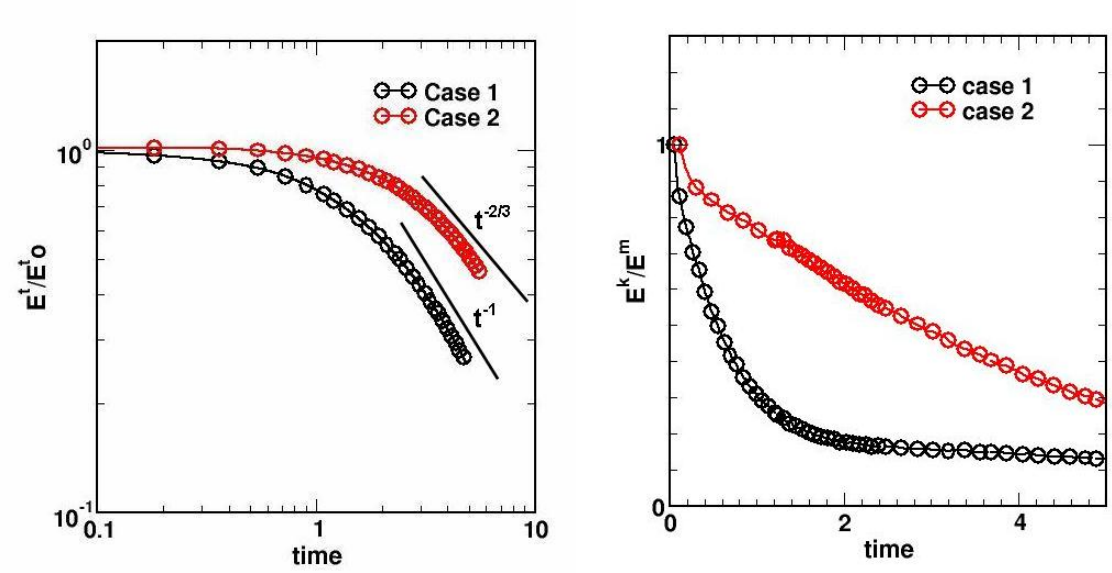

(a) (b)

Figure 10. Time histories of (a)total energy (E^t) and (b) energy ratio (E^k/E^m) for case 1 and 2